

DEDPUL: Difference-of-Estimated-Densities-based Positive-Unlabeled Learning

Dmitry Ivanov

National Research University Higher School of Economics
JetBrains Research
diivanov@hse.ru

Abstract

Positive-Unlabeled (PU) learning is an analog to supervised binary classification for the case when only the positive sample is clean, while the negative sample is contaminated with latent instances of positive class and hence can be considered as an unlabeled mixture. The objectives are to classify the unlabeled sample and train an unbiased PU classifier, which generally requires to identify the mixing proportions of positives and negatives first. Recently, unbiased risk estimation framework has achieved state-of-the-art performance in PU learning. This approach, however, exhibits two major bottlenecks. First, the mixing proportions are assumed to be identified, i.e. known in the domain or estimated with additional methods. Second, the approach relies on the classifier being a neural network. In this paper, we propose DEDPUL, a method that solves PU Learning without the aforementioned issues.¹ The mechanism behind DEDPUL is to apply a computationally cheap post-processing procedure to the predictions of any classifier trained to distinguish positive and unlabeled data. Instead of assuming the proportions to be identified, DEDPUL estimates them alongside with classifying unlabeled sample. Experiments show that DEDPUL outperforms the current state-of-the-art in both proportion estimation and PU Classification.

1 Introduction

PU Classification naturally emerges in numerous real-world cases where obtaining labeled data from both classes is complicated. We informally divide the applications into three categories. In the first category, PU learning is an analog to binary classification. Here, the latter could be applied, but the former accounts for the label noise and hence is more accurate. An example is identification of disease genes. Typically, the already identified disease genes are treated as positive, and the rest unknown genes are treated as negative. Instead,

[Yang *et al.*, 2012] more accurately treat the unknown genes as unlabeled.

In the second category, PU learning is an analog to one-class classification, which learns only from positive data while making assumptions about the negative distribution. For instance, [Blanchard *et al.*, 2010] show that density level set estimation methods [Vert and Vert, 2006; Scott and Nowak, 2006] assume the negative distribution to be uniform, OC-SVM [Schölkopf *et al.*, 2001] finds decision boundary against the origin, and OC-CNN [Oza and Patel, 2018] explicitly models the negative distribution as a Gaussian. Instead, PU learning algorithms approximate the negative distribution as the difference between the unlabeled and the positive, which can be especially crucial when the distributions overlap significantly [Scott and Blanchard, 2009]. Moreover, the outcome of the one-class approach is usually an anomaly metric, whereas PU learning can output unbiased probabilities. Examples are the tasks of anomaly detection, e.g. deceptive reviews [Ren *et al.*, 2014] or fraud [Nguyen *et al.*, 2011].

The third category contains the cases for which neither supervised nor one-class classification could be applied. An example is identification of corruption in Russian procurement auctions [Ivanov and Nesterov, 2019]. An extensive data set of the auctions is available online, however it does not contain any labels of corruption. The proposed solution is to detect only successful corruptioneers by treating runner-ups as fair (positive) and winners as possibly corrupted (unlabeled) participants. PU learning may then detect suspicious patterns based on the subtle differences between the winners and the runner-ups, a task for which one-class approach is too insensitive.

One of the early milestones of PU classification is the paper of [Elkan and Noto, 2008]. The paper makes two major contributions. The first contribution is the notion of Non-Traditional Classifier (NTC), which is any classifier trained to distinguish positive and unlabeled samples. Under the Selected Completely At Random (SCAR) assumption, which states that the labeling probability of any positive instance is constant, the biased predictions of NTC can be transformed into the unbiased posterior probabilities of being positive rather than negative. The second contribution is to consider the unlabeled data as simultaneously positive and negative, weighted by the opposite weights. By substituting these

¹Implementation of DEDPUL is available at <https://github.com/dimonenka/DEDPUL>

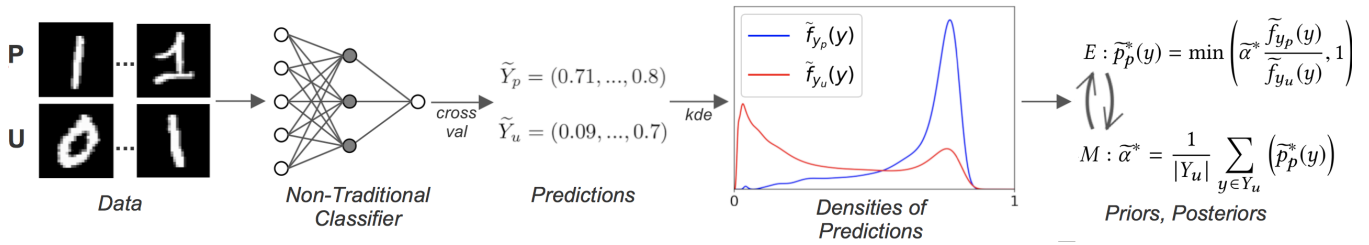


Figure 1: DEDPUL. *Data*: Upper row (ones) represents positive sample X_p , lower row (ones and zeros) represents unlabeled sample X_u . *Non-Traditional Classifier*: NTC is a supervised probabilistic binary classifier trained to distinguish X_p from X_u . *Predictions*: Predicted by NTC probabilities Y_p and Y_u for samples X_p and X_u , obtained with cross-validation. NTC reduces dimensionality. *Densities of Predictions*: Estimated probability density functions $\tilde{f}_{y_p}(y)$ and $\tilde{f}_{y_u}(y)$ on Y_p and Y_u respectively. $\tilde{f}_{y_u}(y)$ has two distinct peaks, one of which coincides with that of $\tilde{f}_{y_p}(y)$, while the other corresponds to the negative component of the mixture. *Priors, Posteriors*: The posteriors are estimated for fixed priors using the Bayes rule and are clipped. The priors are estimated as the average posteriors. These two steps iterate until convergence. If the process converges trivially to 0, an alternative estimate $\tilde{\alpha}_n^*$ is used instead.

weights into the loss function, a PN classifier can be learned directly from PU data. These weights are equal to the posterior probabilities of being positive, estimated based on the predictions of NTC. The idea of loss function reweighting would later be adopted by the Risk Estimation framework [du Plessis *et al.*, 2014; Du Plessis *et al.*, 2015a] and its latest non-negative modification nnPU [Kiryo *et al.*, 2017], which is currently considered state-of-the-art. The crucial insight of this framework is that only the mixing proportion, i.e. the prior probability of being positive, is required to train an unbiased PN classifier on PU data.

While nnPU does not address mixture proportion estimation, multiple studies explicitly focus on this problem [Sanderson and Scott, 2014; Scott, 2015a; du Plessis *et al.*, 2015b]. The state-of-the-art methods are KM [Ramaswamy *et al.*, 2016], which is based on mean embeddings of positive and unlabeled samples into reproducing kernel Hilbert space, and TICe [Bekker and Davis, 2018b], which tries to find a subset of mostly positive data via decision tree induction. Another noteworthy method is AlphaMax [Jain *et al.*, 2016], which explicitly estimates the total likelihood of the data as a function of the proportions and seeks for the point where the likelihood starts to change

This paper makes several distinct contributions. First, we prove that NTC is a posterior-preserving transformation (Section 3.1), whereas NTC is only known in the literature to preserve the priors [Jain *et al.*, 2016]. This enables practical estimation of the posteriors using probability density functions of NTC predictions. Independently, we propose two alternative estimates of the mixing proportions (Section 3.2). These estimates are based on the relation between the priors and the average posteriors. Finally, these new ideas are merged in DEDPUL (Difference-of-Estimated-Densities-based Positive-Unlabeled Learning), a method that simultaneously solves both Mixture Proportions Estimation and PU Classification, outperforms state-of-the-art methods for both problems [Ramaswamy *et al.*, 2016; Bekker and Davis, 2018b; Kiryo *et al.*, 2017], and is applicable to a wide range of mixture proportions and data sets (Section 5).

DEDPUL adheres to the following two-step strategy. At

the first step, NTC is constructed [Elkan and Noto, 2008]. Since NTC treats unlabeled sample as negative, its predictions can be considered as biased posterior probabilities of being positive rather than negative. The second step should eliminate this bias. At the second step, the probability density functions of the NTC predictions for both positive and unlabeled samples are explicitly estimated. Then, both the prior and the posterior probabilities of being positive are estimated simultaneously by plugging these densities into the Bayes rule and performing Expectation-Maximization (EM). In case if EM converges trivially, an alternative algorithm is applied.

2 Problem Setup and Background

In this section, we introduce the notations and formally define the problems of Mixture Proportions Estimation and PU Classification. Additionally, we discuss some of the common assumptions that we use in this work in Section 2.2.

2.1 Preliminaries

Let random variables x_p, x_n, x_u have probability density functions $f_{x_p}(x), f_{x_n}(x), f_{x_u}(x)$ and correspond to positive, negative, and unlabeled distributions of x , where $x \in \mathbb{R}^m$ is a vector of features. Let α be the proportion of $f_{x_p}(x)$ in $f_{x_u}(x)$:

$$f_{x_u}(x) \equiv \alpha f_{x_p}(x) + (1 - \alpha) f_{x_n}(x) \quad (1)$$

Let $p_p(x)$ be the posterior probability that $x \sim f_{x_u}(x)$ is sampled from $f_{x_p}(x)$ rather than $f_{x_n}(x)$. Given the proportion α , it can be computed using the Bayes rule:

$$p_p(x) \equiv \frac{\alpha f_{x_p}(x)}{\alpha f_{x_p}(x) + (1 - \alpha) f_{x_n}(x)} = \alpha \frac{f_{x_p}(x)}{f_{x_u}(x)} \quad (2)$$

2.2 True Proportions are Unidentifiable

The goal of Mixture Proportions Estimation is to estimate the proportions of the mixing components in unlabeled data, given the samples X_p and X_u from the distributions $f_{x_p}(x)$ and $f_{x_u}(x)$ respectively. The problem is fundamentally ill-posed even if the distributions $f_{x_p}(x)$ and $f_{x_u}(x)$ are known.

Algorithm 1 DEDPUL

- 1: **Input:** Unlabeled sample X_u , Positive sample X_p
 - 2: **Output:** Priors $\tilde{\alpha}^*$, Posteriors $\{\tilde{p}_p^*(x) : x \in X_u\}$
 - 3: $\tilde{Y}_u, \tilde{Y}_p = g(X_u), g(X_p) \setminus \setminus$ *NTC predictions*
 - 4: $\tilde{f}_{y_u}(y), \tilde{f}_{y_p}(y) = kde(\tilde{Y}_u), kde(\tilde{Y}_p) \setminus \setminus$ *kernel density estimation*
 - 5: $\tilde{r}(y) = \left\{ \frac{\tilde{f}_{y_p}(y)}{\tilde{f}_{y_u}(y)} : y \in \tilde{Y}_u \right\} \setminus \setminus$ *array of density ratios, assumed to be sorted*
 - 6: $\tilde{r}(y) = \text{MONOTONIZE}(\tilde{r}(y), \tilde{Y}_u) \setminus \setminus$ *enforces partial monotonicity of the ratio curve, defined in Algorithm 2*
 - 7: $\tilde{r}(y) = \text{ROLLING_MEDIAN}(\tilde{r}(y)) \setminus \setminus$ *smooths the ratio curve, defined in Algorithm 2*
 - 8: $\tilde{\alpha}_c^*, \tilde{p}_{p_c}^*(y) = \text{EM}(\tilde{r}(y)); \quad \tilde{\alpha}_n^*, \tilde{p}_{p_n}^*(y) = \text{MAX_SLOPE}(\tilde{r}(y)) \setminus \setminus$ *estimates priors and posteriors, defined in Algorithm 2*
 - 9: **Return** $\tilde{\alpha}_c^*, \tilde{p}_{p_c}^*(y)$ **if** $(\tilde{\alpha}_c^* > 0)$ **else** $\tilde{\alpha}_n^*, \tilde{p}_{p_n}^*(y)$
-

Indeed, based on these densities, a valid estimate of α is any $\tilde{\alpha}$ (tilde denotes estimate) that fits the following constraint from (1):

$$\forall x : f_{x_u}(x) \geq \tilde{\alpha} f_{x_p}(x) \quad (3)$$

In other words, the true proportion α is generally unidentifiable [Blanchard *et al.*, 2010], as it might be any value in the range $\alpha \in [0, \alpha^*]$. However, the upper bound α^* of the range can be identified directly from (3):

$$\alpha^* \equiv \inf_{x \sim f_{x_u}(x)} \frac{f_{x_u}(x)}{f_{x_p}(x)} \quad (4)$$

Denote $p_p^*(x)$ as the corresponding to α^* posteriors:

$$p_p^*(x) \equiv \alpha^* \frac{f_{x_p}(x)}{f_{x_u}(x)} \quad (5)$$

To cope with unidentifiability, a common practice is to make assumptions regarding the proportions, such as mutual irreducibility [Scott *et al.*, 2013] or anchor set [Scott, 2015b; Ramaswamy *et al.*, 2016]. Instead, we consider estimation of the identifiable upper-bound α^* as the objective of Mixture Proportions Estimation, explicitly acknowledging that the true proportion α might be lower. While the two approaches are similar, the distinction becomes meaningful during validation, in particular on synthetic data. In the first approach, the choice of data distributions is limited to the cases where the assumption holds. Otherwise, it might be unclear how to quantify the degree to which the assumption fails and thus its exact effect on misestimation of the proportions. In contrast, the upper-bound α^* can always be computed using equation (4) and taken as a target estimate. We employ this technique in our experiments.

Note that the probability that a positive instance x is labeled is assumed to be constant. This has been formulated in the literature as Selected Completely At Random (SCAR) [Elkan and Noto, 2008]. An emerging alternative is to allow the labeling probability $e(x)$ to depend on the instance, referred to as Selected At Random (SAR) [Bekker and Davis, 2018a]. However, it is easy to see that the priors α^* and the labeling probability $e(x)$ are not uniquely identifiable under SAR without additional assumptions. Specifically, low $f_{x_u}(x)$ compared to $f_{x_p}(x)$ can be explained by either high $e(x)$ or low α^* . Moreover, setting $\frac{e(x)}{1-e(x)} = \frac{f_{x_p}(x)}{f_{x_u}(x)}$ leads

to $\alpha^* = 1$ for any densities. Finding particular assumptions that relax SCAR while maintaining identifiability is an important problem of independent interest [Hammoudeh and Lowd, 2020; Shajarisales *et al.*, 2020]. In this paper, however, we do not aim towards solving this problem. Instead, we propose a novel generic algorithm that assumes SCAR, but can be augmented with less restricting assumptions in the future work.

2.3 Non-Traditional Classifier

Define Non-Traditional Classifier (NTC) as a function $g(x)$:

$$g(x) \equiv \frac{f_{x_p}(x)}{f_{x_p}(x) + f_{x_u}(x)} \quad (6)$$

In practice, NTC is a probabilistic classifier trained on the samples X_p and X_u , balanced by reweighting the loss function. By definition (6), the proportions (4) and the posteriors (5) can be estimated using $g(x)$:

$$\alpha^* = \inf_{x \sim f_{x_u}(x)} \frac{1 - g(x)}{g(x)} \quad (7)$$

$$p_p^*(x) = \alpha^* \frac{g(x)}{1 - g(x)} \quad (8)$$

Directly applying (7) and (8) to the output of NTC has been considered by [Elkan and Noto, 2008] and is referred to as EN method. Its performance is reported in Section 5.2.

Let random variables y_p, y_n, y_u have probability density functions $f_{y_p}(y), f_{y_n}(y), f_{y_u}(y)$ and correspond to the distributions of $y = g(x)$, where $x \sim f_{x_p}(x), x \sim f_{x_n}(x)$, and $x \sim f_{x_u}(x)$ respectively.

3 Algorithm Development

In this section, we propose DEDPUL. The method is summarized in Algorithm 1 and is illustrated in Figure 1, while the secondary functions are presented in Algorithm 2.

In the previous section, we have discussed the case of explicitly known distributions $f_{x_p}(x)$ and $f_{x_u}(x)$. However, only the samples X_p and X_u are usually available. Can we use these samples to estimate the densities $f_{x_p}(x)$ and $f_{x_u}(x)$ and still apply (4) and (5)? Formally, the answer is positive. For proportion estimation, this idea is explored in [Jain *et al.*, 2016] as a baseline. In practice, two crucial issues may arise: the curse of dimensionality and the instability of α^* estimation. We attempt to fix these issues in DEDPUL.

3.1 NTC as Dimensionality Reduction

The first issue is that density estimation is difficult in high dimensions [Liu *et al.*, 2007] and thus the dimensionality should be reduced. To this end, we propose the NTC transformation (6) that reduces the arbitrary number of dimensions to one. Below we prove that it preserves the priors α^* :

$$\alpha^* \equiv \inf_{x \sim f_{x_u}(x)} \frac{f_{x_u}(x)}{f_{x_p}(x)} = \inf_{y \sim f_{y_u}(y)} \frac{f_{y_u}(y)}{f_{y_p}(y)} \quad (9)$$

and the posteriors:

$$p_p^*(x) \equiv \alpha^* \frac{f_{x_p}(x)}{f_{x_u}(x)} = \alpha^* \frac{f_{y_p}(y)}{f_{y_u}(y)} \equiv p_p^*(y) \quad (10)$$

Lemma 1. *NTC is a posterior- and α^* -preserving transformation, i.e. (9) and (10) hold.²*

Proof. To prove (9) and (10), we only need to show that $\frac{f_{x_p}(x)}{f_{x_u}(x)} = \frac{f_{y_p}(y)}{f_{y_u}(y)}$, where $y = g(x)$. We will rely on the rule of variable substitution $f_{y_p}(y) = \sum_{x_r \in r} \frac{f_{x_p}(x_r)}{\nabla g(x_r)}$, where $r = \{x \mid g(x) = y\}$ or, equivalently, $r = \{x \mid \frac{f_{x_p}(x)}{f_{x_u}(x)} = \frac{y}{1-y}\}$:

$$\begin{aligned} \frac{f_{y_p}(y)}{f_{y_u}(y)} &= \frac{\sum_{x_r \in r} \frac{f_{x_p}(x_r)}{\nabla g(x_r)}}{\sum_{x_r \in r} \frac{f_{x_u}(x_r)}{\nabla g(x_r)}} = \frac{\sum_{x_r \in r} \frac{f_{x_p}(x_r)}{\nabla g(x_r)} \frac{f_{x_u}(x_r)}{f_{x_u}(x_r)}}{\sum_{x_r \in r} \frac{f_{x_u}(x_r)}{\nabla g(x_r)} \frac{f_{x_u}(x_r)}{f_{x_u}(x_r)}} \\ &= \frac{y}{1-y} \frac{\sum_{x_r \in r} \frac{f_{x_u}(x_r)}{\nabla g(x_r)}}{\sum_{x_r \in r} \frac{f_{x_u}(x_r)}{\nabla g(x_r)}} = \frac{y}{1-y} = \frac{f_{x_p}(x_r)}{f_{x_u}(x_r)}, x_r \in r \end{aligned}$$

□

Remark on Lemma 1. In the proof, we only use the property of NTC that the density ratio $\frac{f_{x_p}(x)}{f_{x_u}(x)}$ is constant for all x such that $g(x) = y$. Generally, any function $g(x)$ with this property preserves the priors and the posteriors. For instance, NTC could be biased towards 0.5 probability estimate due to regularization. In this case (9) and (10) would still hold, whereas (7) and (8) used in EN would yield incorrect estimates since they rely on NTC being unbiased.

Note that the choice of NTC is flexible. For example, NTC and its hyperparameters can be chosen by maximizing ROC-AUC, a metric that is invariant to label-dependent contamination [Menon *et al.*, 2015; Menon *et al.*, 2016].

After the densities of NTC predictions are estimated, two smoothing heuristics (Algorithm 2) are applied to their ratio.

3.2 Alternative α^* Estimation

The second issue is that (9) may systematically underestimate α^* as it solely relies on the noisy infimum point. This concern is confirmed experimentally in Section 5.2. To resolve it, we propose two alternative estimates. We first prove that these estimates coincide with α^* when the densities are known, and then formulate their practical approximations.

²While (9) is known in the literature [Jain *et al.*, 2016], (10) and the property that $\frac{f_{x_p}(x)}{f_{x_u}(x)} = \frac{f_{y_p}(y)}{f_{y_u}(y)}$ have not been proven before.

Algorithm 2 Secondary functions for DEDPUL

```

1: function EM( $\tilde{r}(y)$ ,  $tol = 10^{-5}$ )
2:    $\tilde{\alpha}^* = 1 \setminus \setminus$  Initialize
3:   repeat
4:      $\tilde{\alpha}_{prev}^* = \tilde{\alpha}^*$ 
5:      $\tilde{p}_p(y) = \min(\tilde{\alpha}^* \cdot \tilde{r}(y), 1) \setminus \setminus$  E-step
6:      $\tilde{\alpha}^* = \frac{1}{|\tilde{Y}_u|} \sum_{y \in \tilde{Y}_u} (\tilde{p}_p(y)) \setminus \setminus$  M-step
7:   until  $|\tilde{\alpha}_{prev}^* - \tilde{\alpha}^*| < tol \setminus \setminus$  Convergence
8:   Return  $\tilde{\alpha}^*, \tilde{p}_p(y)$ 

9: function MAX_SLOPE( $\tilde{r}(y)$ ,  $max\_D = 0.05$ ,  $\epsilon = 10^{-3}$ )
10:   $D = list() \setminus \setminus$  Priors subtract average posteriors
11:  for  $\tilde{\alpha}$  in range(start=0, end=1, step= $\epsilon$ ) do
12:     $\tilde{p}_p(y) = \min(\tilde{\alpha} \cdot \tilde{r}(y), 1)$ 
13:     $idx = \tilde{\alpha} / \epsilon$ 
14:     $D[idx] = \tilde{\alpha} - \frac{1}{|\tilde{Y}_u|} \sum_{y \in \tilde{Y}_u} (\tilde{p}_p(y))$ 
15:   $l = list() \setminus \setminus$  Second lags of D
16:  for  $i$  in range(start=1, end= $\frac{1}{\epsilon} - 1$ , step=1) do
17:     $l[i] = (D[i-1] - D[i]) / \epsilon - (D[i] - D[i+1])$ 
18:   $\tilde{\alpha}^* = argmax(l)$  s. t.  $D < max\_D$ 
19:   $\tilde{p}_p(y) = \min(\tilde{\alpha}^* \cdot \tilde{r}(y), 1)$ 
20:  Return  $\tilde{\alpha}^*, \tilde{p}_p(y)$ 

21: function MONOTONIZE( $\tilde{r}(y)$ ,  $\tilde{Y}_u$ )
22:   $max_{cur} = 0$ ,  $threshold = \frac{1}{|\tilde{Y}_u|} \sum_{\tilde{y} \in \tilde{Y}_u} \tilde{y}$ 
23:  for  $i$  in range(start=0, end=length( $\tilde{r}(y)$ ), step=1) do
24:    if  $\tilde{Y}_u[i] \geq threshold$  then
25:       $max_{cur} = \max(\tilde{r}(y)[i], max_{cur})$ 
26:       $\tilde{r}(y)[i] = max_{cur}$ 
27:  Return  $\tilde{r}(y)$ 

28: function ROLLING_MEDIAN( $\tilde{r}(y)$ )
29:   $L = length(\tilde{r}(y))$ ,  $k = L/20$ 
30:   $\tilde{r}_{new}(y) = \tilde{r}(y)$ 
31:  for  $i$  in range(start=0, end=L, step=1) do
32:     $k_{cur} = \min(k, i, L-i) \setminus \setminus$  Number of neighbours
33:     $\tilde{r}_{new}(y)[i] = median(\tilde{r}(y)[i - k_{cur} : i + k_{cur}])$ 
34:  Return  $\tilde{r}_{new}(y)$ 

```

Lemma 2. *Alternative estimates of the priors are equal to the definition (9): $\alpha_c^* = \alpha_n^* = \alpha^*$, where*

$$D(\alpha) \equiv \alpha - \mathbb{E}_{y \sim f_{y_u}(y)} [p_p(y)],$$

$$\alpha_c^* \equiv \max_{\alpha \in [0,1]} \{\alpha \mid D(\alpha) = 0\},$$

$$\alpha_n^* \equiv \min_{\alpha \in [0,1]} \{\alpha \mid D(\alpha + \epsilon) - 2D(\alpha) + D(\alpha - \epsilon) > 0\}.$$

Proof. We first prove that $D(\alpha)$ behaves in a specific way (Fig. 2a). For the valid priors $\alpha \leq \alpha^*$, it holds that $D(\alpha) = 0$, since priors must be equal to expected posteriors: $p(h) = \mathbb{E}_{x \sim f(x)} p(h \mid x)$ for some hypothesis h and data $x \sim f(x)$.

For the invalid priors $\alpha > \alpha^*$, the situation changes. By definition of α^* (9), it is now the case that $p_p(y) = \alpha \frac{f_{y_p}(y)}{f_{y_u}(y)} > 1$ for some y . To prevent this, the posteriors are clipped from above like in (11). Under this redefinition, the equality of priors to expected posteriors no longer holds. Instead, clipping decreases the posteriors in comparison to the priors. Thus, for

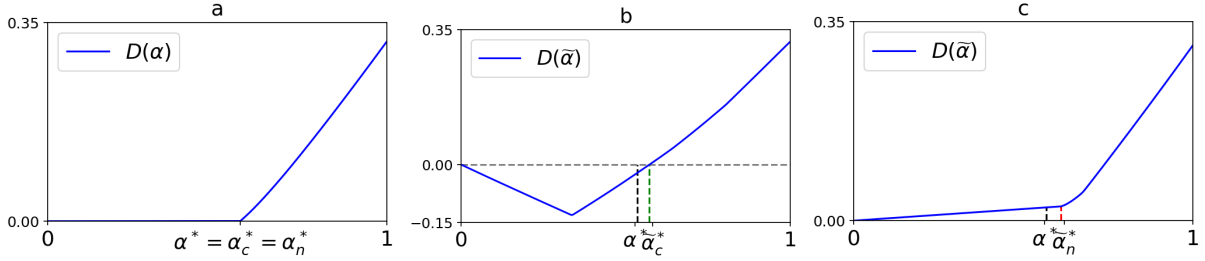


Figure 2: Behaviours of $D(\alpha)$ in theory (a) and practice (b, c). In these plots, $f_{x_p}(x) = L(0, 1)$, $f_{x_n} = L(2, 1)$, $\alpha = 0.5$, and $\alpha^* = 0.568$, where $L(\cdot, \cdot)$ denotes Laplace distribution.

$\alpha > \alpha^*$ it holds that $\alpha > \mathbb{E}_{y \sim f_{y_u}(y)} [p_p(y)]$ and $D(\alpha) > 0$.

So, $D(\alpha)$ equals 0 up until α^* and is positive after. It trivially follows that α^* is the highest α for which $D(\alpha) = 0$, and the lowest α for which $D(\alpha + \epsilon) - 2 \cdot D(\alpha) + D(\alpha - \epsilon) = D(\alpha + \epsilon) > 0$ for any ϵ (in practice, ϵ is chosen small). \square

Figures 2b and 2c reflect how $D(\alpha)$ changes in practice due to imperfect density estimation: in simple words, the curve either ‘rotates’ down or up. In the more frequent first case, non-trivial $\tilde{\alpha}_c^*$ exists (the curve intersects zero). We identify it using Expectation-Maximization algorithm, but analogs like binary search could be used as well. In the second case (e.g. sometimes when α^* is extremely low), non-trivial $\tilde{\alpha}_c^*$ does not exist and EM converges to $\tilde{\alpha} = 0$. In this case, we instead approximate $\tilde{\alpha}_n^*$ using MAX_SLOPE function. We define these functions in Algorithm 2 and cover them below in more details. In DEDPUL, the two estimates are switched by choosing the maximal. In practice, we recommend to plot $D(\alpha)$ to visually identify α_c^* (if exists) or α_n^* .

Approximation of α_c^* with EM algorithm. On Expectation step, the proportion $\tilde{\alpha}$ is fixed and the posteriors $\tilde{p}_p(y)$ are estimated using clipped (10):

$$\tilde{p}_p(y) = \min \left(\tilde{\alpha} \frac{\tilde{f}_{y_p}(y)}{\tilde{f}_{y_u}(y)}, 1 \right) \quad (11)$$

On Maximization step, $\tilde{\alpha}$ is updated as the average value of the posteriors over the unlabeled sample \tilde{Y}_u :

$$\tilde{\alpha} = \frac{1}{|\tilde{Y}_u|} \sum_{y \in \tilde{Y}_u} (\tilde{p}_p(y)) \quad (12)$$

These two steps iterate until convergence. The algorithm should be initialized with $\tilde{\alpha} = 1$.

Approximation of α_n^* with MAX_SLOPE. On a grid of proportion values $\tilde{\alpha} \in [0, 1]$, second difference of $D(\tilde{\alpha})$ is calculated for each point. Then, the proportion that corresponds to the highest second difference is chosen.

4 Experimental Procedure

We conduct experiments on synthetic and benchmark data sets. Although DEDPUL is able to solve both Mixture Proportions Estimation and PU Classification simultaneously,

some of the algorithms are not. For this reason, all PU Classification algorithms receive α^* (synthetic data) or α (benchmark data) as an input. The algorithms are tested on numerous data sets that differ in the distributions and the proportions of the mixing components. Additionally, each experiment is repeated 10 times, and the results are averaged.

The statistical significance of the difference between the algorithms is verified in two steps. First, the Friedman test with 0.02 P-value threshold is applied to check whether all the algorithms perform equivalently. If this null hypothesis is rejected, the algorithms are compared pair-wise using the paired Wilcoxon signed-rank test with 0.02 P-value threshold and Holm correction for multiple hypothesis testing. The results are summarized via critical difference diagrams (Fig. 3), the code for which is taken from [Ismail Fawaz *et al.*, 2019].

4.1 Data

In the synthetic setting we experiment with mixtures of one-dimensional Laplace distributions. We fix $f_{x_p}(x)$ as $L(0, 1)$ and mix it with different $f_{x_n}(x)$: $L(1, 1)$, $L(2, 1)$, $L(4, 1)$, $L(0, 2)$, $L(0, 4)$. For each of these cases, the proportion α is varied in $\{0.01, 0.05, 0.25, 0.5, 0.75, 0.95, 0.99\}$. The sample sizes X_p and X_u are fixed as 1000 and 10000.

In the benchmark setting (Table 1) we experiment with eight data sets from UCI machine learning repository [Bache and Lichman, 2013], MNIST image data set of handwritten digits [LeCun *et al.*, 2010], and CIFAR-10 image data set of vehicles and animals [Krizhevsky *et al.*, 2009]. The proportion α is varied in $\{0.05, 0.25, 0.5, 0.75, 0.95\}$. The methods’ performance is mostly determined by the size of the labeled sample $|X_p|$. Therefore, for a given data set, $|X_p|$ is fixed across the different values of α , and for a given α , the maximal $|X_u|$ that can satisfy it is chosen. Categorical features are transformed using dummy encoding. Numerical features are normalized. Regression and multi-classification target variables are adapted for binary classification.

4.2 Measures for Performance Evaluation

The synthetic setting provides a straightforward way to evaluate performance. Since the underlying distributions $f_{x_p}(x)$ and $f_{x_u}(x)$ are known, we calculate the true values of the proportions α^* and the posteriors $p_p^*(x)$ using (4) and (5) respectively. Then, we directly compare these values with algorithm’s estimates using mean absolute errors. In the benchmark setting, the distributions are unknown. Here, for Mix-

data set	total size	$ X_p $	dim	positive target
bank	45211	1000	16	yes
concrete	1030	100	8	(35.8, 82.6)
landsat	6435	1000	36	4, 5, 7
mushroom	8124	1000	22	p
pageblock	5473	100	10	2, 3, 4, 5
shuttle	58000	1000	9	2, 3, 4, 5, 6, 7
spambase	4601	400	57	1
wine	6497	500	12	red
mnist	70000	1000	784	1, 3, 5, 7, 9
cifar10	60000	1000	3072	plane, car ship, track

Table 1: Description of benchmark data sets

ture Proportions Estimation we use a similar measure, but substitute α^* with α , while for PU Classification we use $1 - accuracy$ with 0.5 probability threshold. We additionally compare the algorithms using f1-measure, a popular metric for imbalanced data sets.

4.3 Implementations of Methods

DEDPUL is implemented according to Algorithms 1 and 2. As NTC we apply neural networks with 1 hidden layer with 16 neurons (1-16-1) to the synthetic data, and with 2 hidden layers with 512 neurons (dim-512-512-1) and with batch normalization [Ioffe and Szegedy, 2015] after the hidden layers to the benchmark data. To CIFAR-10, a light version of all-convolutional net [Springenberg *et al.*, 2015] with 6 convolutional and 2 fully-connected layers is applied, with 2-d batch normalization after the convolutional layers. These architectures are used henceforth in EN and nnPU. The networks are trained on the logistic loss with ADAM [Kingma and Ba, 2015] optimizer with 0.0001 weight decay. The predictions of each network are obtained with 5-fold cross-validation.

Densities of the predictions are computed using kernel density estimation with Gaussian kernels. Instead of $\tilde{y} \in [0, 1]$, we estimate densities of appropriately ranged $\log\left(\frac{\tilde{y}}{1-\tilde{y}}\right)$ and make according post-transformations. Bandwidths are set as 0.1 and 0.05 for $\tilde{f}_{y_p}(y)$ and $\tilde{f}_{y_u}(y)$ respectively. In practice, a well-performing heuristic is to independently choose bandwidths for $\tilde{f}_{y_p}(y)$ and $\tilde{f}_{y_u}(y)$ that maximize average log-likelihood during cross-validation. Threshold in MONOTONIZE is chosen as $\frac{1}{|X_u|} \sum_{x \in X_u} (\tilde{g}(x))$.

The implementations of the Kernel Mean based gradient thresholding algorithm (KM) are retrieved from the original paper [Ramaswamy *et al.*, 2016].³ We provide experimental results for KM2, a better performing version. As advised in the paper, MNIST and CIFAR-10 data are reduced to 50 dimensions with Principal Component Analysis [Wold *et al.*, 1987]. Since KM2 cannot handle big data sets, it is applied to subsamples of at most 4000 examples (X_p is prioritized).

The implementation of Tree Induction for label frequency c Estimation (TICe) algorithm is retrieved from the original

paper [Bekker and Davis, 2018b].⁴ MNIST and CIFAR-10 data are reduced to 200 dimensions with Principal Component Analysis. In addition to the vanilla version, we also apply TICe to the data preprocessed with NTC (NTC+TICe). The performance of both versions heavily depends on the choice of the hyperparameters such as the probability lower bound δ and the number of splits per node s . These parameters were chosen as $\delta = 0.2$ and $s = 40$ for univariate data, and $\delta = 0.2$ and $s = 4$ for multivariate data.

We explore two versions of the non-negative PU learning (nnPU) algorithm [Kiryo *et al.*, 2017]: the original version with Sigmoid loss function and our modified version with Brier loss function.⁵ The hyperparameters were chosen as $\beta = 0$ and $\gamma = 1$ for the benchmark data, and as $\beta = 0.1$ and $\gamma = 0.9$ for the synthetic data.

Elkan-Noto (EN) is implemented according to the original paper [Elkan and Noto, 2008]. Out of the three proposed estimators of the labeling probability, we report results for e_3 (equivalent to (7)) since it has shown better performance.

5 Experimental results

5.1 Comparison with State-of-the-art

Results of comparison between DEDPUL and state-of-the-art are presented in Figures 4-7 and are summarized in Figure 3. DEDPUL significantly outperforms state-of-the-art of both problems in both setups for all measures, with the exception of insignificant difference between f1-measures of DEDPUL and nnPU-sigmoid in the benchmark setup.

On some benchmark data sets (Fig. 5 – landsat, pageblock, wine), KM2 performs on par with DEDPUL for all α values except for the highest $\alpha = 0.95$, while on the other data sets (except for bank) KM2 is strictly outmatched. The regions of low proportion of negatives are of special interest in the anomaly detection task, and it is a vital property of an algorithm to find anomalies that are in fact present. Unlike DEDPUL, TICe, and EN, KM2 fails to meet this requirement. On the synthetic data (Fig. 4) DEDPUL also outperforms KM2, especially when the priors are high.

Regarding comparison with TICe, DEDPUL outperforms both its vanilla and NTC versions in both synthetic and benchmark settings (Fig. 4, 5). Two insights about TICe could be noted. First, while the NTC preprocessing is redundant for one-dimensional synthetic data, it can greatly improve the performance of TICe on the high-dimensional benchmark data, especially on image data. Second, while KM2 generally performs a little better than TICe on the synthetic data, the situation is reversed on the benchmark data.

In the posteriors estimation task, DEDPUL matches or outperforms both Sigmoid and Brier versions of nnPU algorithm on all data sets in both setups (Fig. 6, 7). An insight about the Sigmoid version is that it estimates probabilities relatively poorly (Fig. 6). This is because the Sigmoid loss is minimized by the median prediction, i.e. either 0 or 1 label, while the Brier loss is minimized by the average prediction, i.e. a

⁴<https://dtai.cs.kuleuven.be/software/tice>

⁵Sigmoid and Brier loss functions are mean absolute and mean squared errors between classifier’s predictions and true labels.

³<http://web.eecs.umich.edu/~cscott/code.html#kmp2>.

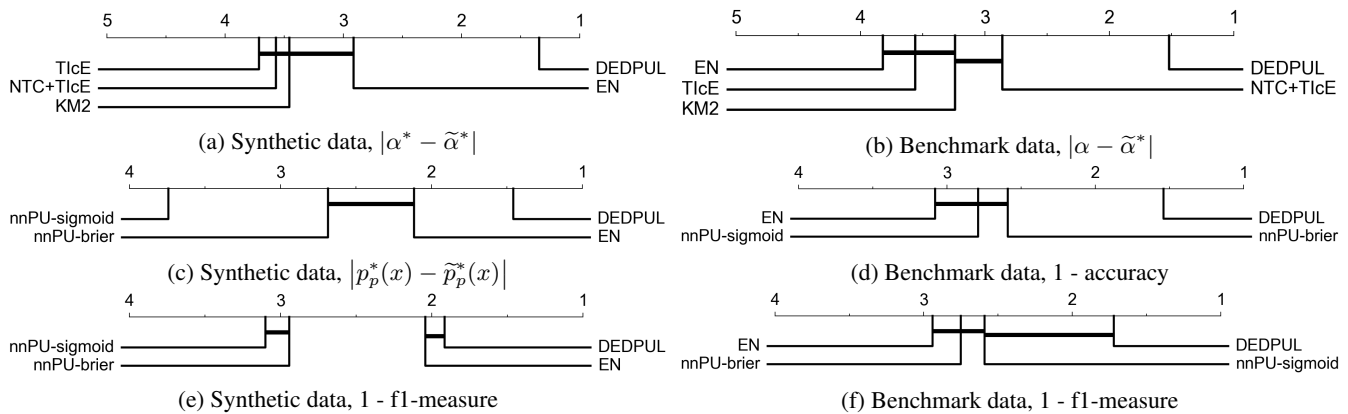


Figure 3: Critical difference diagrams. Summarized comparison of the algorithms on synthetic and benchmark data with different performance measures. The horizontal axis represents relative ranking. Bold horizontal lines represent statistically insignificant differences. In the synthetic setup, accuracy differs insignificantly between the algorithms according to the Friedman test, so the diagram is not reported.

probability in $[0, 1]$ range. Conversely, there is no clear winner in the benchmark setting (Fig. 7). On some data sets (bank, concrete, landsat, pageblock, spambase) the Brier loss leads to the better training, whereas on other data sets (mushroom, shuttle, wine, mnist) the Sigmoid loss prevails.

Below we show that the performance of DEDPUL can be further improved by the appropriate choice of NTC.

5.2 Ablation study

DEDPUL is a combination of multiple parts such as NTC, density estimation, EM algorithm, and several heuristics. To disentangle the contribution of these parts to the overall performance of the method, we perform an ablation study. We modify different details of DEDPUL and report changes in performance in Figures 8-11.

First, we vary NTC. Instead of neural networks, we try gradient boosting of decision trees. We use an open-source library *CatBoost* [Prokhorenkova *et al.*, 2018]. For the synthetic and the benchmark data respectively, the height of the trees is limited to 4 and 8, and the learning rate is chosen as 0.1 and 0.01; the amount of trees is defined by early stopping.

Second, we vary density estimation methods. Aside from default kernel density estimation (*kde*), we try Gaussian Mixture Models (*GMM*) and histograms (*hist*). The number of gaussians for GMM is chosen as 20 and 10 for $f_u(x)$ and $f_p(x)$ respectively, and the number of bins for histograms is chosen as 20 for both densities.

Third, we replace the proposed estimates of priors α_c^* and α_n^* with the default estimate (9) (*simple_alpha*). This is similar to the pdf-ratio baseline from [Jain *et al.*, 2016]. We replace infimum with 0.05 quantile for improved stability.

Fourth, we remove MONOTONIZE and ROLLING_MEDIAN heuristics that smooth the density ratio (*no_smooth*).

Fifth, we report performance of *EN* method [Elkan and Noto, 2008]. This can be seen as ablation of DEDPUL where density estimation is removed altogether and is replaced by simpler equations (7) and (8).

CatBoost. In the synthetic setting, CatBoost is outmatched by neural networks as NTC on both tasks (Fig. 8, 10). The sit-

uation changes in the benchmark setting, where CatBoost outperforms neural networks on most data sets, especially during label assignment (Fig. 11). Still, neural networks are a better choice for image data sets. This comparison highlights the flexibility in the choice of NTC for DEDPUL depending on the data at hand.

Density estimation. On the task of proportion estimation in the synthetic data, *kde* performs a little better than analogues. However, the choice of the density estimation procedure has little effect with no clear trend in other setups (Fig. 9-11), which indicates robustness of DEDPUL to the choice.

Default α^* . On all data sets, using the default α^* estimation method (9) massively degrades the performance, especially when contamination of the unlabeled sample with positives is high (Fig. 8, 9). This is to be expected, since the estimate (9) is a single infimum (or low quantile) point of the noisy density ratio, while the alternatives leverage the entire unlabeled sample. Thus, the proposed estimates α_c^* and α_n^* are vital for DEDPUL stability.

No smoothing. While not being very impactful on the estimation of posteriors, the smoothing heuristics are vital for the quality of the proportion estimation (Fig. 8, 9).

EN. In the synthetic setup, performance of EN is decent (Fig. 4, 6). It outperforms both versions of Tlce on most and nnPU-sigmoid on all synthetic data sets. In the benchmark setup, EN is the worst procedure for proportion estimation (Fig. 5), but it still outperforms nnPU on some data sets (concrete, landsat, shuttle, spambase) during label assignment (Fig. 7). Nevertheless, EN never surpasses DEDPUL, except for $L(0, 2)$. The striking difference between the two methods might be explained with EN requiring more from NTC, as discussed in Section 3.1.

6 Conclusion

In this paper, we have proven that NTC is a posterior-preserving transformation, proposed an alternative method of proportion estimation based on $D(\alpha)$, and combined these

findings in DEDPUL. We have conducted an extensive experimental study to show superiority of DEDPUL over current state-of-the-art in Mixture Proportion Estimation and PU Classification. DEDPUL is applicable to a wide range of mixing proportions, is flexible in the choice of the classification algorithm, is robust to the choice of the density estimation procedure, and overall outperforms analogs.

There are several directions to extend our work. Despite our theoretical finding, the reasons behind the behaviour of $D(\alpha)$ in practice remain unclear. In particular, we are uncertain why non-trivial α_c^* does not exist in some cases and what distinguishes these cases. Next, it could be valuable to explore the extensions of DEDPUL to the related problems such as PU multi-classification or mutual contamination. Another promising topic is relaxation of SCAR. Finally, modifying DEDPUL with variational inference might help to internalize density estimation into the classifier's training procedure.

Acknowledgements

I sincerely thank Alexander Nesterov, Alexander Sirotkin, Iskander Safulin, Ksenia Balabaeva and Vitalia Eliseeva for regular revisions of the paper. Support from the Basic Research Program of the National Research University Higher School of Economics is gratefully acknowledged.

References

- [Bache and Lichman, 2013] K. Bache and M. Lichman. UCI machine learning repository, 2013.
- [Bekker and Davis, 2018a] Jessa Bekker and Jesse Davis. Beyond the selected completely at random assumption for learning from positive and unlabeled data. *arXiv preprint arXiv:1809.03207*, 2018.
- [Bekker and Davis, 2018b] Jessa Bekker and Jesse Davis. Estimating the class prior in positive and unlabeled data through decision tree induction. In *Proceedings of the 32th AAAI Conference on Artificial Intelligence*, 2018.
- [Blanchard *et al.*, 2010] Gilles Blanchard, Gyemin Lee, and Clayton Scott. Semi-supervised novelty detection. *Journal of Machine Learning Research*, 11(Nov):2973–3009, 2010.
- [du Plessis *et al.*, 2014] Marthinus C du Plessis, Gang Niu, and Masashi Sugiyama. Analysis of learning from positive and unlabeled data. In *Advances in neural information processing systems*, pages 703–711, 2014.
- [Du Plessis *et al.*, 2015a] Marthinus Du Plessis, Gang Niu, and Masashi Sugiyama. Convex formulation for learning from positive and unlabeled data. In *International Conference on Machine Learning*, pages 1386–1394, 2015.
- [du Plessis *et al.*, 2015b] Marthinus Christoffel du Plessis, Gang Niu, and Masashi Sugiyama. Class-prior estimation for learning from positive and unlabeled data. In *ACML*, pages 221–236, 2015.
- [Elkan and Noto, 2008] Charles Elkan and Keith Noto. Learning classifiers from only positive and unlabeled data. In *Proceedings of the 14th ACM SIGKDD international conference on Knowledge discovery and data mining*, pages 213–220. ACM, 2008.
- [Hammoudeh and Lowd, 2020] Zayd Hammoudeh and Daniel Lowd. Learning from positive and unlabeled data with arbitrary positive shift. *arXiv preprint arXiv:2002.10261*, 2020.
- [Ioffe and Szegedy, 2015] Sergey Ioffe and Christian Szegedy. Batch normalization: Accelerating deep network training by reducing internal covariate shift. In *International Conference on Machine Learning*, pages 448–456, 2015.
- [Ismail Fawaz *et al.*, 2019] Hassan Ismail Fawaz, Germain Forestier, Jonathan Weber, Lhassane Idoumghar, and Pierre-Alain Muller. Deep learning for time series classification: a review. *Data Mining and Knowledge Discovery*, 33(4):917–963, 2019.
- [Ivanov and Nesterov, 2019] Dmitry I Ivanov and Alexander S Nesterov. Identifying bid leakage in procurement auctions: Machine learning approach. *arXiv preprint arXiv:1903.00261*, 2019.
- [Jain *et al.*, 2016] Shantanu Jain, Martha White, Michael W Trosset, and Predrag Radivojac. Nonparametric semi-supervised learning of class proportions. *arXiv preprint arXiv:1601.01944*, 2016.
- [Kingma and Ba, 2015] Diederik P Kingma and Jimmy Ba. Adam: A method for stochastic optimization. *International Conference for Learning Representations*, 2015.
- [Kiryo *et al.*, 2017] Ryuichi Kiryo, Gang Niu, Marthinus C du Plessis, and Masashi Sugiyama. Positive-unlabeled learning with non-negative risk estimator. In *Advances in Neural Information Processing Systems*, pages 1675–1685, 2017.
- [Krizhevsky *et al.*, 2009] Alex Krizhevsky, Geoffrey Hinton, et al. Learning multiple layers of features from tiny images. Technical report, Citeseer, 2009.
- [LeCun *et al.*, 2010] Yann LeCun, Corinna Cortes, and CJ Burges. MNIST handwritten digit database. *AT&T Labs [Online]*. Available: <http://yann.lecun.com/exdb/mnist>, 2, 2010.
- [Liu *et al.*, 2007] Han Liu, John Lafferty, and Larry Wasserman. Sparse nonparametric density estimation in high dimensions using the rodeo. In *Artificial Intelligence and Statistics*, pages 283–290, 2007.
- [Menon *et al.*, 2015] Aditya Menon, Brendan Van Rooyen, Cheng Soon Ong, and Bob Williamson. Learning from corrupted binary labels via class-probability estimation. In *International Conference on Machine Learning*, pages 125–134, 2015.
- [Menon *et al.*, 2016] Aditya Krishna Menon, Brendan Van Rooyen, and Nagarajan Natarajan. Learning from binary labels with instance-dependent corruption. *arXiv preprint arXiv:1605.00751*, 2016.
- [Nguyen *et al.*, 2011] Minh Nhut Nguyen, Xiaoli-Li Li, and See-Kiong Ng. Positive unlabeled learning for time se-

- ries classification. In *IJCAI*, volume 11, pages 1421–1426, 2011.
- [Oza and Patel, 2018] Poojan Oza and Vishal M Patel. One-class convolutional neural network. *IEEE Signal Processing Letters*, 26(2):277–281, 2018.
- [Prokhorenkova *et al.*, 2018] Liudmila Prokhorenkova, Gleb Gusev, Aleksandr Vorobev, Anna Veronika Dorogush, and Andrey Gulin. Catboost: unbiased boosting with categorical features. In *Advances in Neural Information Processing Systems*, pages 6638–6648, 2018.
- [Ramaswamy *et al.*, 2016] Harish Ramaswamy, Clayton Scott, and Ambuj Tewari. Mixture proportion estimation via kernel embeddings of distributions. In *International Conference on Machine Learning*, pages 2052–2060, 2016.
- [Ren *et al.*, 2014] Yafeng Ren, Donghong Ji, and Hongbin Zhang. Positive unlabeled learning for deceptive reviews detection. In *EMNLP*, pages 488–498, 2014.
- [Sanderson and Scott, 2014] Tyler Sanderson and Clayton Scott. Class proportion estimation with application to multiclass anomaly rejection. In *Artificial Intelligence and Statistics*, pages 850–858, 2014.
- [Schölkopf *et al.*, 2001] Bernhard Schölkopf, John C Platt, John Shawe-Taylor, Alex J Smola, and Robert C Williamson. Estimating the support of a high-dimensional distribution. *Neural computation*, 13(7):1443–1471, 2001.
- [Scott and Blanchard, 2009] Clayton Scott and Gilles Blanchard. Novelty detection: Unlabeled data definitely help. In *Artificial Intelligence and Statistics*, pages 464–471, 2009.
- [Scott and Nowak, 2006] Clayton D Scott and Robert D Nowak. Learning minimum volume sets. *Journal of Machine Learning Research*, 7(Apr):665–704, 2006.
- [Scott *et al.*, 2013] Clayton Scott, Gilles Blanchard, and Gregory Handy. Classification with asymmetric label noise: Consistency and maximal denoising. In *Conference On Learning Theory*, pages 489–511, 2013.
- [Scott, 2015a] Clayton Scott. A rate of convergence for mixture proportion estimation, with application to learning from noisy labels. In *Artificial Intelligence and Statistics*, pages 838–846, 2015.
- [Scott, 2015b] Clayton Scott. A rate of convergence for mixture proportion estimation, with application to learning from noisy labels. In *Artificial Intelligence and Statistics*, pages 838–846, 2015.
- [Shajarisales *et al.*, 2020] Naji Shajarisales, Peter Spirtes, and Kun Zhang. Learning from positive and unlabeled data by identifying the annotation process. *arXiv preprint arXiv:2003.01067*, 2020.
- [Springenberg *et al.*, 2015] Jost Tobias Springenberg, Alexey Dosovitskiy, Thomas Brox, and Martin Riedmiller. Striving for simplicity: The all convolutional net. *International Conference for Learning Representations Workshop*, 2015.
- [Vert and Vert, 2006] Régis Vert and Jean-Philippe Vert. Consistency and convergence rates of one-class svms and related algorithms. *Journal of Machine Learning Research*, 7(May):817–854, 2006.
- [Wold *et al.*, 1987] Svante Wold, Kim Esbensen, and Paul Geladi. Principal component analysis. *Chemometrics and intelligent laboratory systems*, 2(1-3):37–52, 1987.
- [Yang *et al.*, 2012] Peng Yang, Xiao-Li Li, Jian-Ping Mei, Chee-Keong Kwoh, and See-Kiong Ng. Positive-unlabeled learning for disease gene identification. *Bioinformatics*, 28(20):2640–2647, 2012.

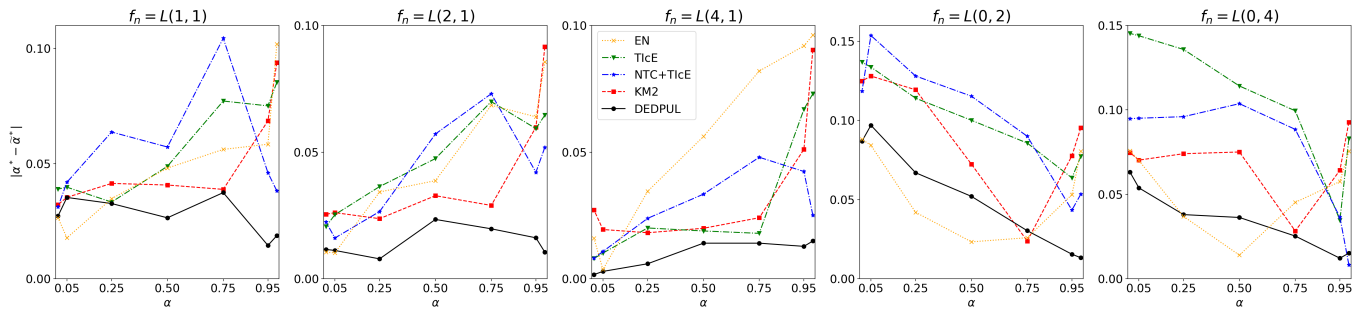


Figure 4: Comparison of Mixture Proportions Estimation Algorithms, Synthetic Data

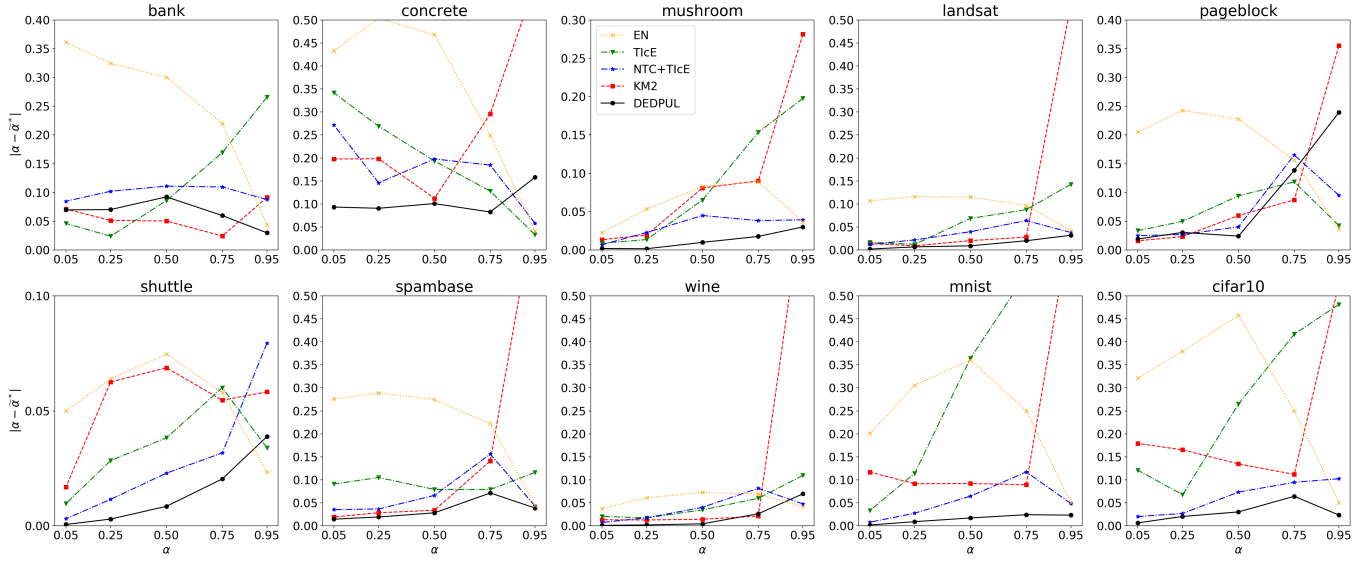


Figure 5: Comparison of Mixture Proportions Estimation Algorithms, Benchmark Data

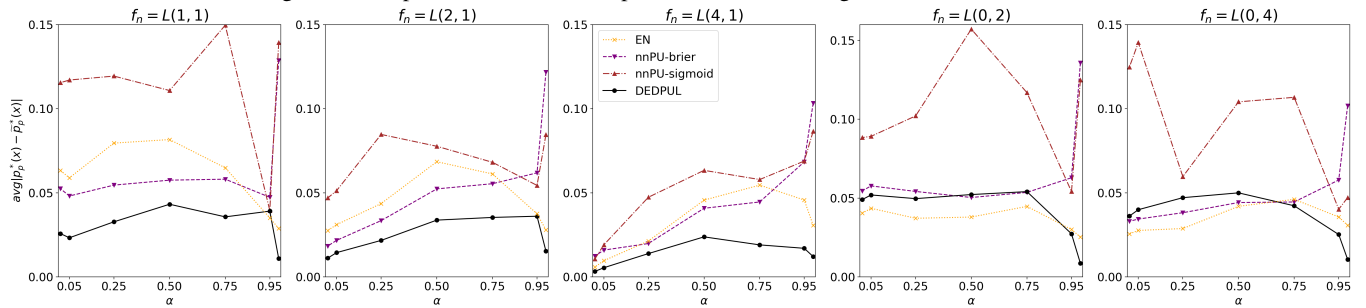


Figure 6: Comparison of Positive-Unlabeled Classification Algorithms, Synthetic Data

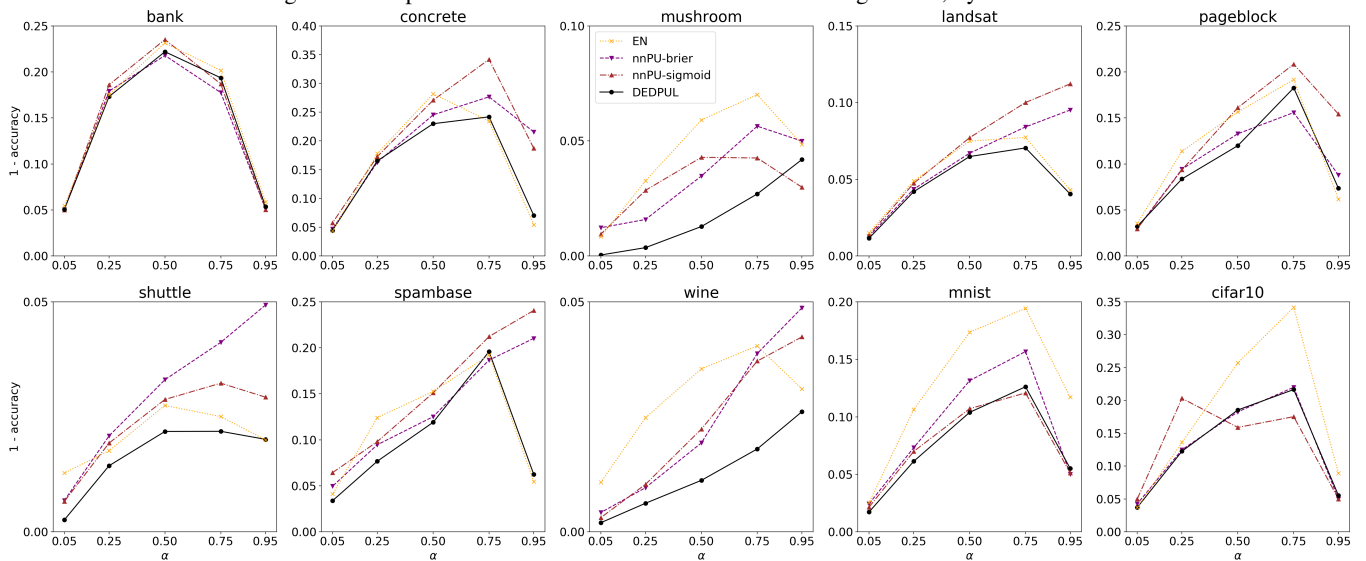


Figure 7: Comparison of Positive-Unlabeled Classification Algorithms, Benchmark Data

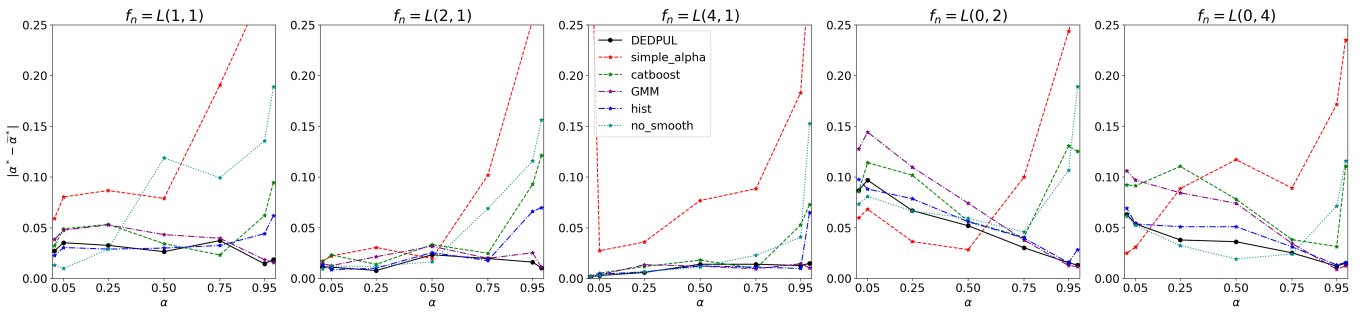


Figure 8: Ablations of DEDPUL, Mixture Proportions Estimation, Synthetic Data

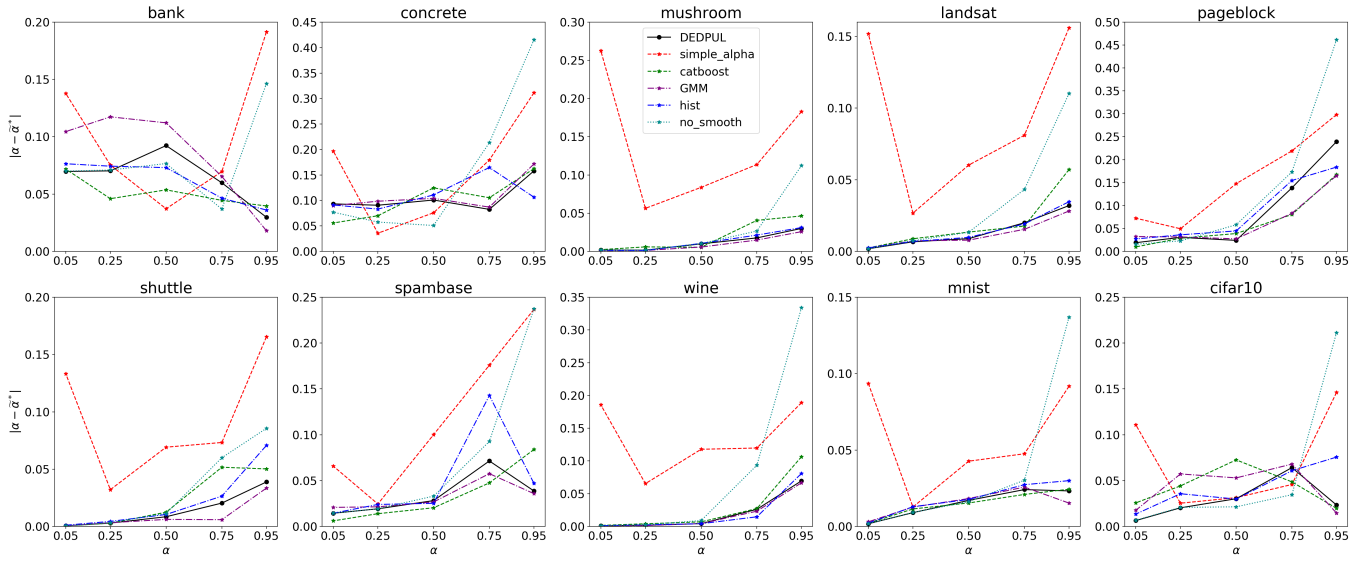


Figure 9: Ablations of DEDPUL, Mixture Proportions Estimation, Benchmark Data

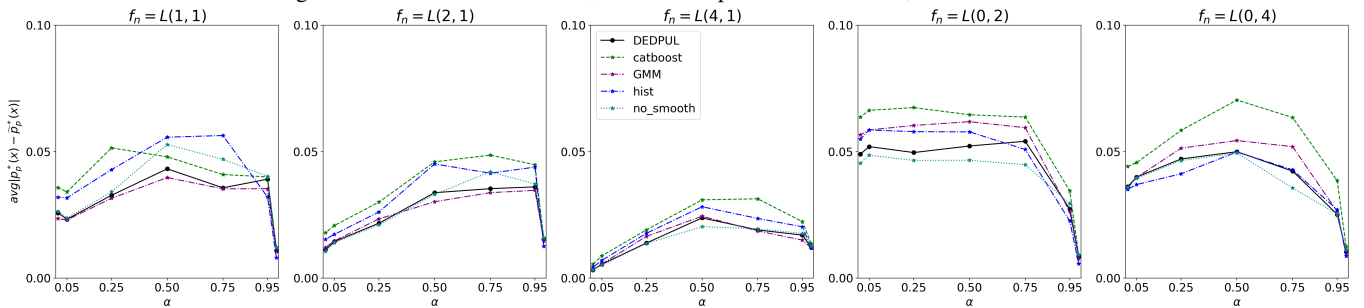


Figure 10: Ablations of DEDPUL, Positive-Unlabeled Classification, Synthetic Data

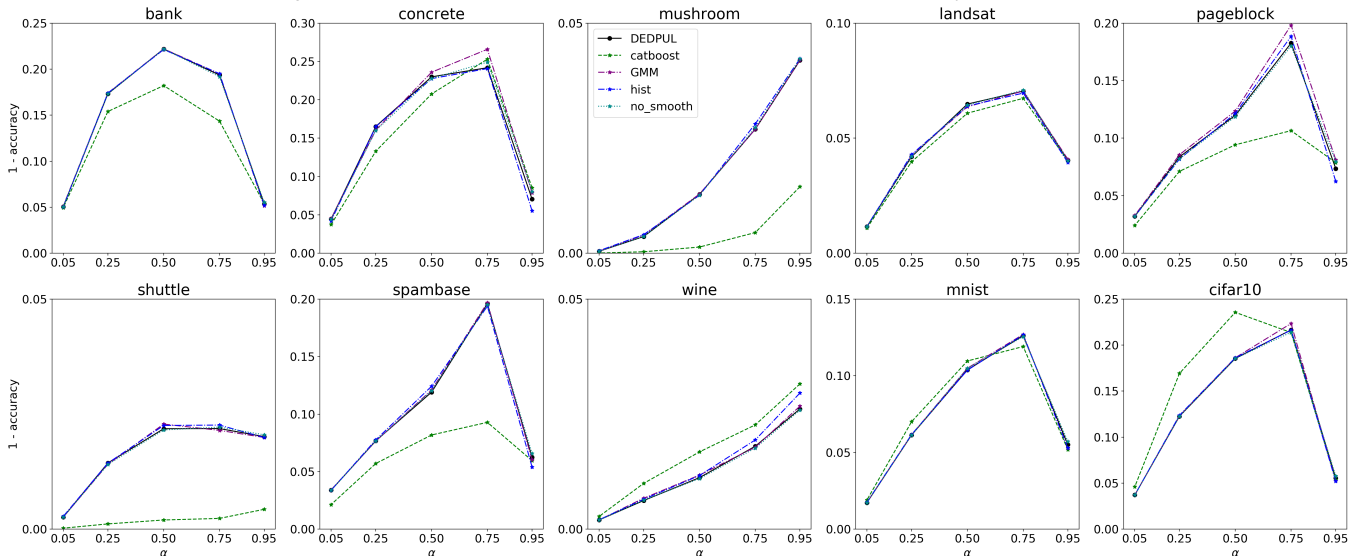


Figure 11: Ablations of DEDPUL, Positive-Unlabeled Classification, Benchmark Data